Testing J/ψ production and decay properties in hadronic collisions

E. Mirkes
Department of Physics, University of Wisconsin, Madison, Wisconsin 53706

C. S. Kim
Department of Physics, Yonsei University, Seoul 120-749, Korea
(Received 11 October 1994)

The polar and azimuthal angular distributions for the lepton pair arising from the decay of a J/ψ meson produced at transverse momentum p_T balanced by a photon (or gluon) in hadronic collisions are calculated in the color singlet model (CSM). It is shown that the general structure of the decay lepton distribution is controlled by four invariant structure functions, which are functions of the transverse momentum and the rapidity of the J/ψ. We find that two of these structure functions (the longitudinal and transverse interference structure functions) are identical in the CSM. Analytical and numerical results are given in the Collins-Soper and in the Gottfried-Jackson frames. We present a Monte Carlo study of the effect of acceptance cuts applied to the leptons and the photon for $J/\psi+\gamma$ production at the Fermilab Tevatron.

PACS number(s): 13.85.Qk, 13.20.Gd, 14.40.Gx

I. INTRODUCTION

The study of the properties of the bound states of heavy quarks plays a central role in the understanding of perturbative quantum chromodynamics. In addition to the intrinsic interest in the bound state properties of a J/ψ, the study of the ${}^3S_1 - c\bar{c}$ bound state is also of particular importance in the measurement of b quark production. So far there have been intensive experimental studies of the J/ψ production rate and transverse momentum distributions in hadronic collisions both at UA1 [1] and the Collider Detector at Fermilab (CDF) [2]. However, the observed J/ψ rate was found to be markedly higher than the predicted ones in [3], where in addition to the direct charmonium production also contributions from the χ and the production resulting from B decays were taken into account. It has recently been pointed out in [4] that at large transverse momentum of the J/ψ an additional production mechanism comes from fragmentation contributions of a gluon or a charm quark into charmonium states.

In this paper we propose to measure the decay lepton distribution of the J/ψ as a detailed test of the production mechanism of the $c\bar{c}$ bound state. We restrict ourselves in the present paper to the study of J/ψ produced in association with a photon. This has several advantages. First, the experimental signature of a J/ψ (decaying into an e^-e^+ or $\mu^-\mu^+$ pair) and a γ with balancing transverse momentum is a very clean final state. Second, the fragmentation contributions [5] or contributions from radiative χ decays[1] to $J/\psi + \gamma$ production are small and the dominant subprocess contributing to a $J/\psi + \gamma$ final state is the gluon-gluon fusion process.

For J/ψ's produced with transverse momentum p_T (balanced by the additional photon) one can define an event plane spanned by the beam and the J/ψ momentum direction which provides a reference plane for a detailed study of angular correlations. The decay lepton distribution in $J/\psi \to l^-l^+$ in the J/ψ rest frame is determined by the polarization of the J/ψ. Therefore, the study of the angular distribution can be used as an analyzer of the J/ψ polarization. It is thus possible to test the underlying J/ψ production dynamics [in our case the color singlet model (CSM) [6]] in much more detail than is possible by rate measurements alone. It is shown that the angular distribution of the leptons in the J/ψ rest frame has the general form

$$\sigma \sim (1+\cos\theta^2) + \frac{1}{2}A_0\,(1-3\cos^2\theta) + A_1\,\sin 2\theta\cos\phi + \frac{1}{2}A_2\,\sin^2\theta\cos 2\phi\,, \tag{1}$$

where θ and ϕ denote the polar and azimuthal angle of the decay leptons in the J/ψ rest frame. The coefficients A_i in Eq. (1) are functions of the transverse momentum and rapidity of the J/ψ. We present analytical results for these coefficients in the Collins-Soper (CS) [7] and Gottfried-Jackson (GJ) frames. The functions A_0 and A_2 are found to be equal in the CSM. An experimental analyses of this equality would be a sensitive test of the CSM. We show numerical results for the transverse momentum $[p_T(J/\psi)]$ and rapidity $[y(J/\psi)]$ dependence of the coefficients A_i and study the effect of the acceptance cuts on the ϕ and $\cos\theta$ distributions in the CS and GJ frame.

The coefficients A_i are ratios of helicity cross sections [see Eq. (28)] and the uncertainties from higher order QCD corrections and the wave function of the bound state are expected to cancel in this ratio. This has been shown for the related process of high p_T lepton pair production in the Drell-Yan process [8], where large QCD

[1]The radiative χ_J decays can produce J/ψ at both low and high p_T, but the photon produced will be soft [$E \sim 400$ MeV].

corrections to the individual helicity cross sections almost cancel in the corresponding ratios $A_i^{\rm DY}$. A similar effect is expected in the case of J/ψ production and our leading order (LO) predictions for the A_i and the [normalized] ϕ and $\cos\theta$ distributions provide therefore a useful test of J/ψ production.

Our analytical results for the coefficients A_i are also valid for $J/\psi + g$ production within the CSM. As mentioned before, there are additional fragmentation contributions of a gluon or a charm quark to this final state [4]. The polarization dependence of the J/ψ from these contributions has recently been discussed in [9]. A study of the angular distribution as proposed in this paper may allow disentangling the different contributions.

Recently, J/ψ's produced in association with a photon have been proposed as a clean probe to study the gluon distribution and the polarized gluon distribution of proton as well as to investigate qualitatively the production mechanism of heavy quark bound states [10]. An investigation of the decay lepton distribution and structure functions of J/ψ's production and decay in e^-e^+– experiments is presented in [11].

The remainder of this paper is organized as follows: In Sec. II, analytical results for the helicity cross sections and the coefficients A_i are derived in the CSM for the CS and GJ frames and the formalism for describing the angular distributions is discussed. Numerical results are presented in Sec. III and summary remarks are given in Sec. IV. Some technical details of the calculation are relegated to the Appendix.

II. STRUCTURE FUNCTIONS AND ANGULAR DISTRIBUTIONS

We consider the angular distribution of the leptons coming from the leptonic decay of J/ψ's produced with nonzero transverse momentum in association with a photon in high energy proton-antiproton collisions. For definiteness we take

$$p(P_1) + \bar{p}(P_2) \to J/\psi(P) + \gamma(k) + X \to l^-(l) + l^+(l') + \gamma(k) + X \,, \tag{2}$$

where the quantities in the parentheses denote the four-momenta. In leading order of perturbative QCD [$O(\alpha_s^2)$], $J/\psi + \gamma$ can only be produced in gg fusion:

$$g(p_1) + g(p_2) \to J/\psi(P) + \gamma(k) \,. \tag{3}$$

In the parton model the hadronic cross section is obtained by folding the hard parton level cross section with the respective parton densities:

$$\frac{d\sigma^{h_1 h_2}}{dp_T^2\, dy\, d\Omega^*} = \int dx_1 dx_2 g^{h_1}(x_1,\mu_F^2) g^{h_2}(x_2,\mu_F^2) \times \frac{s\, d\hat{\sigma}}{dt\, du\, d\Omega^*}(x_1 P_1, x_2 P_2, \alpha_s(\mu_R^2)) \,, \tag{4}$$

where $g^h(x,\mu_F^2)$ is the probability density to find a gluon with fraction x in hadron h if it is probed at a scale μ_F^2. The partonic cross section for the process in Eq. (3) is denoted by $d\hat{\sigma}$. Denoting hadron level and parton level quantities by upper and lower case characters, respectively, the hadron and parton level Mandelstam variables are defined by

$$S = (P_1 + P_2)^2 \,, \qquad T = (P_1 - P)^2 \,, \qquad U = (P_2 - P)^2 \,, \tag{5}$$

and

$$\begin{aligned} s &= (p_1 + p_2)^2 = x_1 x_2 S \,, \\ t &= (p_1 - P)^2 = x_1 (T - P^2) + P^2 \,, \\ u &= (p_2 - P)^2 = x_2 (U - P^2) + P^2 \,, \end{aligned} \tag{6}$$

where $p_1 = x_1 P_1$ and $p_2 = x_1 P_2$. The rapidity y of the J/ψ in the laboratory frame can be written as

$$y = \frac{1}{2} \ln\left(\frac{P^2 - U}{P^2 - T}\right) \,, \tag{7}$$

and the transverse momentum of the J/ψ is related to the Mandelstam variables via

$$p_T^2 = \frac{(P^2 - U)(P^2 - T)}{S} - P^2 = \frac{ut}{s} \,. \tag{8}$$

The angles θ and ϕ in $d\Omega^* = d\cos\theta\, d\phi$ in Eq. (4) are the polar and azimuthal decay angles of the leptons in the J/ψ rest frame with respect to a coordinate system described below. The angular dependence in (4) can be extracted by introducing four helicity cross sections corresponding to the four nonzero combinations of polarization density matrix elements (see Appendix A of this paper, and Appendix C of [8] for details):

$$\frac{16\pi}{3} \frac{d\sigma}{dp_T^2\, dy\, d\cos\theta\, d\phi} = \frac{d\sigma^{U+L}}{dp_T^2\, dy}(1 + \cos^2\theta) + \frac{d\sigma^L}{dp_T^2\, dy}(1 - 3\cos^2\theta) + \frac{d\sigma^T}{dp_T^2\, dy} 2\sin^2\theta\cos 2\phi + \frac{d\sigma^I}{dp_T^2\, dy} 2\sqrt{2}\sin 2\theta\cos\phi \,. \tag{9}$$

The hadronic helicity cross sections $\frac{d\sigma^\alpha}{dp_T^2\, dy}$ are again obtained by convoluting the partonic helicity cross sections with the gluon densities. One has

$$\frac{d\sigma^\alpha}{dp_T^2\, dy} = \int dx_1 dx_2 g^{h_1}(x_1,\mu_F^2) g^{h_2}(x_2,\mu_F^2) \frac{s\, d\hat{\sigma}^\alpha}{dt\, du} \,. \tag{10}$$

Each of the partonic helicity cross sections is calculated in the CSM. The unpolarized differential production cross section is denoted by $\hat{\sigma}^{U+L}$ whereas $\hat{\sigma}^{L,T,I}$ characterize the polarization of the J/ψ, i.e., the cross section for the longitudinal polarized J/ψ's is denoted by $\hat{\sigma}^L$, the transverse-longitudinal interference by $\hat{\sigma}^I$, and the trans-

verse interference by $\hat{\sigma}^T$ [see. Eq. (A9); all with respect to the z axis of the chosen J/ψ rest frame]. The results for the helicity cross sections $\hat{\sigma}^\alpha$ are dependent of the choice of the z axis in the rest frame of the J/ψ. We will derive explicit results for the Collins-Soper (CS) and the Gottfried-Jackson (GJ) frames.

In the CS frame [7] the z axis bisects the angle between $\vec{P}_1$ and $-\vec{P}_2$:

$$\begin{aligned} \text{CS}: \quad \vec{P}_1 &= E_1\ (\sin\gamma_{\text{CS}}, 0, \cos\gamma_{\text{CS}})\ , \\ \vec{P}_2 &= E_2\ (\sin\gamma_{\text{CS}}, 0, -\cos\gamma_{\text{CS}})\ , \end{aligned} \tag{11}$$

with

$$\cos\gamma_{\text{CS}} = \sqrt{\frac{{m_\psi}^2 S}{(T-{m_\psi}^2)(U-{m_\psi}^2)}} = \sqrt{\frac{{m_\psi}^2}{{m_\psi}^2+p_T^2}}\ , \tag{12}$$

$$\sin\gamma_{\text{CS}} = -\sqrt{1-\cos^2\gamma_{\text{CS}}}\ . \tag{13}$$

In the GJ frame (also known as t-channel helicity frame) the z axis is chosen parallel to the beam axis:

$$\begin{aligned} \text{GJ}: \quad \vec{P}_1 &= E_1\ (0,0,1)\ , \\ \vec{P}_2 &= E_2\ (\sin\gamma_{\text{GJ}}, 0, \cos\gamma_{\text{GJ}})\ , \end{aligned} \tag{14}$$

with

$$\cos\gamma_{\text{GJ}} = 1 - \frac{2{m_\psi}^2 S}{(T-{m_\psi}^2)(U-{m_\psi}^2)} = \frac{p_T^2-{m_\psi}^2}{p_T^2+{m_\psi}^2}\ , \tag{15}$$

$$\sin\gamma_{\text{GJ}} = -\sqrt{1-\cos^2\gamma_{\text{GJ}}}\ . \tag{16}$$

The beam and target energies for both rest frames are

$$E_1 = ({m_\psi}^2 - T)/(2m_\psi), \quad E_2 = ({m_\psi}^2 - U)/(2m_\psi)\ .$$

The partonic helicity cross sections in Eq. (10) are calculated applying the technique described in [8] to the CSM (see Appendix A for details). They are given by

$$\begin{aligned} \frac{s\hat{\sigma}^\alpha_{\text{CS,GJ}}}{dtdu} &= \frac{16\pi\alpha\alpha_s^2 m_\psi}{27s}|R(0)|^2 \\ &\quad \times H^\alpha_{\text{CS,GJ}}\,\delta(s+t+u-{m_\psi}^2)\ , \end{aligned} \tag{17}$$

with

$$\begin{aligned} H^{U+L}_{\text{CS}} &= \frac{s^2}{(t-{m_\psi}^2)^2(u-{m_\psi}^2)^2} \\ &\quad + \frac{t^2}{(u-{m_\psi}^2)^2(s-{m_\psi}^2)^2} \\ &\quad + \frac{u^2}{(s-{m_\psi}^2)^2(t-{m_\psi}^2)^2}\ , \end{aligned} \tag{18}$$

$$\begin{aligned} H^L_{\text{CS}} &= \frac{ut}{2(t-{m_\psi}^2)(u-{m_\psi}^2)} \\ &\quad \times\left(\frac{4{m_\psi}^2 s^3}{(s-{m_\psi}^2)^2(t-{m_\psi}^2)^2(u-{m_\psi}^2)^2} + H^{U+L}_{\text{CS}}\right), \end{aligned} \tag{19}$$

$$H^T_{\text{CS}} = \frac{1}{2}H^L_{\text{CS}}\ , \tag{20}$$

$$H^I_{\text{CS}} = \frac{m_\psi\sqrt{sut}\ \ s(s^2-ut)(t-u)}{\sqrt{2}(s-{m_\psi}^2)^2(t-{m_\psi}^2)^3(u-{m_\psi}^2)^3}\ , \tag{21}$$

and, for the GJ frame,

$$H^{U+L}_{\text{GJ}} = H^{U+L}_{\text{CS}}\ , \tag{22}$$

$$H^L_{\text{GJ}} = \frac{2{m_\psi}^2 stu(s^2+u^2)}{(s-{m_\psi}^2)^2(t-{m_\psi}^2)^4(u-{m_\psi}^2)^2}\ , \tag{23}$$

$$H^T_{\text{GJ}} = \frac{1}{2}H^L_{\text{GJ}}\ , \tag{24}$$

$$H^I_{\text{GJ}} = -\frac{m_\psi\sqrt{stu}\,(s-u)[s^2(u-t)+u^2(s-t)]}{\sqrt{2}(s-{m_\psi}^2)^2(t-{m_\psi}^2)^4(u-{m_\psi}^2)^2}\ . \tag{25}$$

As mentioned before, H^{U+L} denotes the matrix element contribution for the production rate and was first calculated in [12]. All other matrix elements correspond to the production of *polarized* J/ψ's and are given here for the first time. Replacing 16α by $15\alpha_s$ in Eq. (17), the results in Eqs. (17)–(25) are also valid for $J/\psi + g$ production within the CSM.

Note, that the matrix elements can be expressed in terms of p_T^2, y by noting that

$$\begin{aligned} t &= {m_\psi}^2 - \sqrt{({m_\psi}^2+p_T^2)S}\ x_1 e^{-y}\ , \\ u &= {m_\psi}^2 - \sqrt{({m_\psi}^2+p_T^2)S}\ x_2 e^{y}\ , \end{aligned} \tag{26}$$

so that, e.g.,

$$\begin{aligned} \frac{({m_\psi}^2-t)({m_\psi}^2-u)}{s} &= p_T^2+{m_\psi}^2\ , \\ \text{and also} \quad \frac{ut}{s} &= p_T^2\ . \end{aligned} \tag{27}$$

From the explicit expressions in Eqs. (18)–(25) one observes that the longitudinal and the transverse interference cross sections σ^L and σ^T are related by $\sigma_L = 2\sigma_T$ and that they vanish for $p_T \to 0$ with p_T^2. The longitudinal-transverse interference cross section σ^I vanishes with p_T, whereas the production cross section σ^{U+L} for unpolarized J/ψ's is finite in the $p_T \to 0$ limit.

Introducing standard angular coefficients [7]

$$A_0 = \frac{2\ d\sigma^L}{d\sigma^{U+L}}\ , \quad A_1 = \frac{2\sqrt{2}\ d\sigma^I}{d\sigma^{U+L}}\ , \quad A_2 = \frac{4\ d\sigma^T}{d\sigma^{U+L}}\ , \tag{28}$$

the angular distribution of Eq. (9) is conveniently written as

$$\frac{d\sigma}{dp_T^2\, dy\, d\cos\theta\, d\phi} = \frac{3}{16\pi}\frac{d\sigma^{U+L}}{dp_T^2\, dy}\left[(1+\cos^2\theta) + \frac{1}{2}A_0\ (1-3\cos^2\theta) + A_1\ \sin 2\theta\cos\phi\ + \frac{1}{2}A_2\ \sin^2\theta\cos 2\phi\right]. \tag{29}$$

Integrating the angular distribution in Eq. (29) over the azimuthal angle ϕ yields

$$\frac{d\sigma}{dp_T^2\, dy\, d\cos\theta} = C\,(1+\alpha\cos^2\theta)\,, \tag{30}$$

where

$$C = \frac{3}{8}\frac{d\sigma^{U+L}}{dp_T^2\, dy}\left[1+\frac{A_0}{2}\right], \quad \alpha = \frac{2-3A_0}{2+A_0}\,. \tag{31}$$

And integration over θ yields

$$\frac{d\sigma}{dp_T^2\, dy\, d\phi} = \frac{1}{2\pi}\frac{d\sigma^{U+L}}{dp_T^2\, dy}(1+\beta\cos 2\phi)\,, \tag{32}$$

where

$$\beta = \frac{A_2}{4}\,. \tag{33}$$

Before discussing numerical results, let us briefly discuss a possibility strategy for extracting angular coefficients. By taking moments with respect to an appropriate product of trigonometric functions it is possible to disentangle the coefficients A_i. A convenient definition of the moments through

$$\langle m\rangle = \frac{\int d\sigma(p_T,y,\theta,\phi)\ m\ d\cos\theta\, d\phi}{\int d\sigma(p_T,y,\theta,\phi)\ d\cos\theta\, d\phi}\,, \tag{34}$$

which leads to the results

$$\langle 1\rangle = 1\,, \tag{35}$$

$$\langle \tfrac{1}{2}(1-3\cos^2\theta)\rangle = \frac{3}{20}\left(A_0 - \frac{2}{3}\right), \tag{36}$$

$$\langle \sin 2\theta\cos\phi\rangle = \frac{1}{5}\,A_1\,, \tag{37}$$

$$\langle \sin^2\theta\cos 2\phi\rangle = \frac{1}{10}\,A_2\,. \tag{38}$$

III. NUMERICAL RESULTS

We will now present numerical results for $J/\psi + \gamma$ production at the Fermilab Tevatron collider center of mass energy [$\sqrt{S} = 1.8$ TeV] including the decay $J/\psi \to \mu^-\mu^+$. All results are obtained using the gluon density parametrization from Glück, Reya, and Vogt (GRV) [13] with $\Lambda^{(4)}_{\overline{\rm MS}} = 200$ MeV and the one-loop formula for α_s with four active flavors, where $\overline{\rm MS}$ denotes the modified minimal subtraction scheme. If not stated otherwise, we identify the renormalization scale μ_R^2 and the factorization scale μ_F^2 in Eq. (4) and set them equal to $\mu^2 = \mu_F^2 = \mu_R^2 = [m_\psi{}^2 + p_T^2(J/\psi)]$. The value for the bound state wave function at the origin $|R(0)|^2$ is determined from the leptonic decay width of J/ψ: $\Gamma(J/\psi \to e^-e^+) = 4.72$ keV, therefore $|R(0)|^2 = 0.48$ GeV^3.

Figure 1 shows the transverse momentum distribution of the the J/ψ where we have applied the cuts $|y(\gamma,l^-,l^+)| < 2.5$ and $p_T(l^-,l^+) > 1.8$ GeV on the final state particles. The p_T distributions are leading order predictions and are therefore strongly dependent on the choice of the scales μ^2 and the radial wave function of the bound state. In fact, the New Muon Collaboration (NMC) found [14] that the LO predictions describes the shape of all kinematical variables quite well, while the predictions for the normalization of the signal was too small by a factor 2–3. This large "K factor" is probably due to the nonrelativistic treatment of the J/ψ and due to higher order QCD corrections in the CSM. One can expect a similar K factor for our reaction, so that our result of Fig. 1 should be considered as conservative estimates. To give a feeling for the scale dependence we show results for $\mu^2 = \mu_F^2 = \mu_R^2 = [m_\psi{}^2 + p_T^2(J/\psi)]$

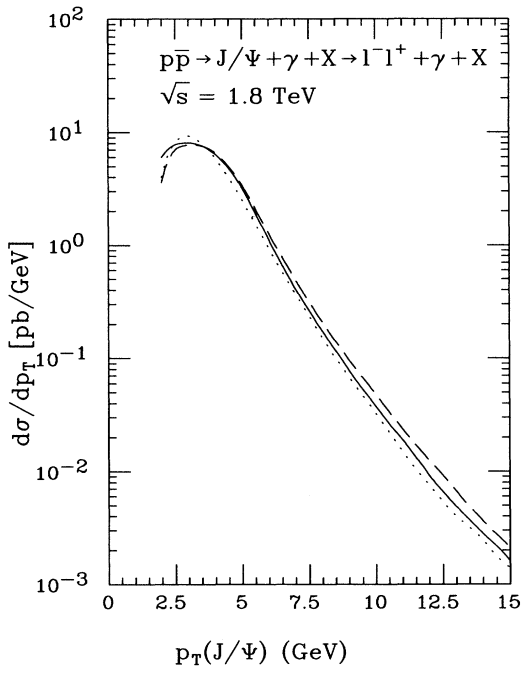

FIG. 1. The transverse momentum distribution of the J/ψ [or γ] in $J/\psi + \gamma$ production at the Tevatron collider center of mass energy [$\sqrt{S} = 1.8$ TeV] with subsequent $J/\psi \to \mu^-\mu^+$ decay. The following cuts have been applied: $|y(\gamma,l^-,l^+)| < 2.5$ and $p_T(l^-,l^+) > 1.8$ GeV. The renormalization and factorization scales μ^2 are set equal to $(p_T^2(\gamma) + m_\psi{}^2)$ [solid], $\frac{1}{4}\,(p_T^2(\gamma) + m_\psi{}^2)$ [dashed] and $4\,(p_T^2(\gamma) + m_\psi{}^2)$ [dotted].

[solid line], $\mu^2 = [{m_\psi}^2 + p_T^2(J/\psi)]/4$ [dashed line], and $\mu^2 = 4[{m_\psi}^2 + p_T^2(J/\psi)]$ [dotted line].

Figure 2 shows the rapidity distribution of the photon normalized to the total production cross section. The following cuts are applied: $p_T(\gamma, l^-, l^+) > 3$ GeV. The shape of this distribution is quite sensitive to the gluon density function, and therefore useful to extract the gluon density at the small x [10].

In Fig. 3, we show the transverse momentum distributions of the decay leptons from the J/ψ after the cuts: $|y(\gamma, l^-, l^+)| < 2.5$, $p_T(l^-, l^+) > 1.8$ GeV and $p_T(\gamma) > 2$ GeV. We also plot the spectrum of the harder (denoted by b) and softer (denoted by s) lepton separately, where we did not distinguish between the charge of the leptons. Note that together with the hard photon, this harder lepton (denoted by b) can be used to construct a trigger for our reaction. As in Fig. 1, the p_T distributions of the leptons are strongly dependent on the choice of the scales μ^2 and the radial wave function of the bound state.

In Figs. 4 and 5 we show numerical results for the coefficients A_i in Eq. (29) as a function of $p_T(J/\psi)$ and $y(J/\psi)$ in the CS [Figs. 4 and 5(a)] and GJ [Figs. 4 and 5(b)] frame. These coefficients have been extracted from the Monte Carlo program by using the moments defined in Eq. (34). No acceptance cuts have been applied to the leptons or the photon. One observes that the coefficients are strongly dependent on $p_T(J/\psi)$ both in the CS and GJ frame. As mentioned before, the coefficients A_0 and A_2 are exactly equal in lowest order in both lepton pair rest frames. The angular coefficient A_1 is zero in the CS frame for all values of $p_T(J/\psi)$. The reason is that the matrix element for A_1 is antisymmetric in u and t [see Eqs. (21) and (28)] and therefore in x_1 and x_2, whereas the product of the gluon distributions is symmetric under the interchange of x_1 and x_2. As a consequence, the rapidity distribution for A_1 in the CS frame [Fig. 5(a)] is also antisymmetric around $y = 0$. However, this is different for the GJ frame [see Eq. (25)]. All coefficients A_i vanish in the limit $p_T(J/\psi) \to 0$, which can be directly seen from our analytical expressions in Eqs. (18)–(25) and 28).

A similar relation $A_0^{\mathrm{DY}} = A_2^{\mathrm{DY}}$ was found in LO $[O(\alpha_s)]$ in the Drell-Yan process [15] $p + \bar{p} \to V + X \to l^+ l' + X$, where V denotes a gauge boson produced at high p_T. In [8], the complete next to LO (NLO) corrections to the coefficients A_i^{DY} are calculated and the corrections are found to be fairly small for the ratios A_i of the corresponding helicity cross section. We expect also here, that the LO results for the ratios A_i in J/ψ production are almost not affected by higher order QCD corrections. Note also, that the coefficients A_i are not dependent on the bound state wave function. The measurement of these coefficients would be a sensitive test of the production mechanism of J/ψ's. However, as we will see later, experimental cuts introduce additional complicated angular effects and the resulting data sample can

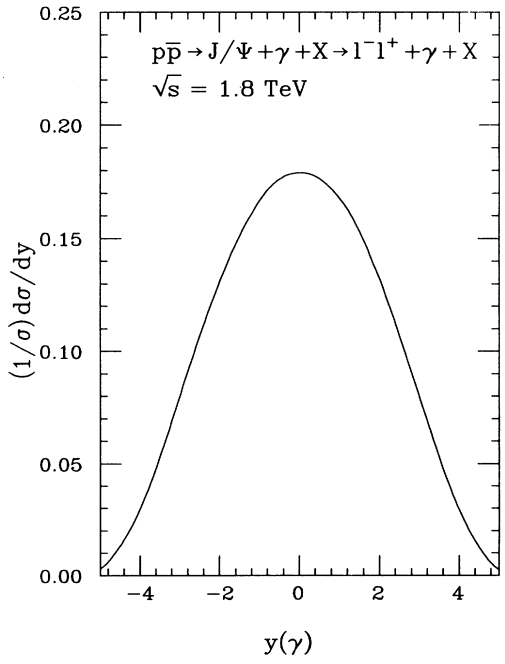

FIG. 2. The normalized rapidity distribution of the γ in $J/\psi + \gamma$ production at the Tevatron collider center-of-mass energy [$\sqrt{S} = 1.8$ TeV] with subsequent $J/\psi \to \mu^-\mu^+$ decay. The following cuts have been applied: $p_T(\gamma, l^-, l^+) > 3$ GeV.

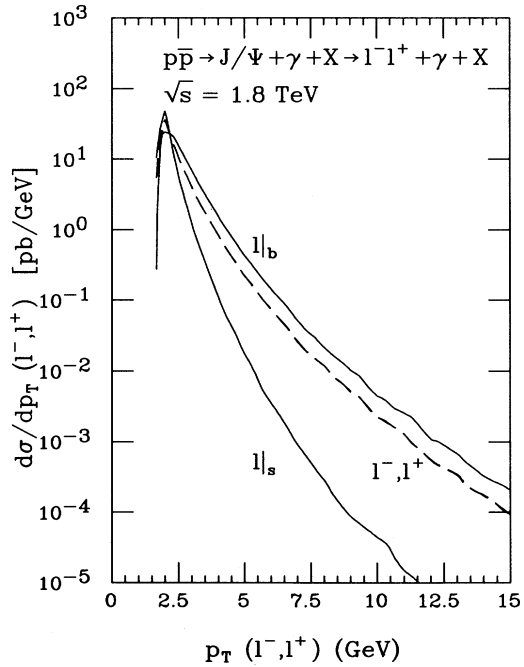

FIG. 3. The transverse momentum distribution of the leptons from the decay of the J/ψ in $J/\psi + \gamma$ production at the Tevatron collider center-of-mass energy [$\sqrt{S} = 1.8$ TeV]. The following cuts have been applied: $|y(\gamma, l^-, l^+)| < 2.5$, $p_T(l^-, l^+) > 1.8$ GeV and $p_T(\gamma) > 2$ GeV. Results are shown for the positive (negative) charged lepton (dashed lines) as well as the distribution for the lepton with bigger (subscript b) and smaller (subscript s) p_T without identifying the charge.

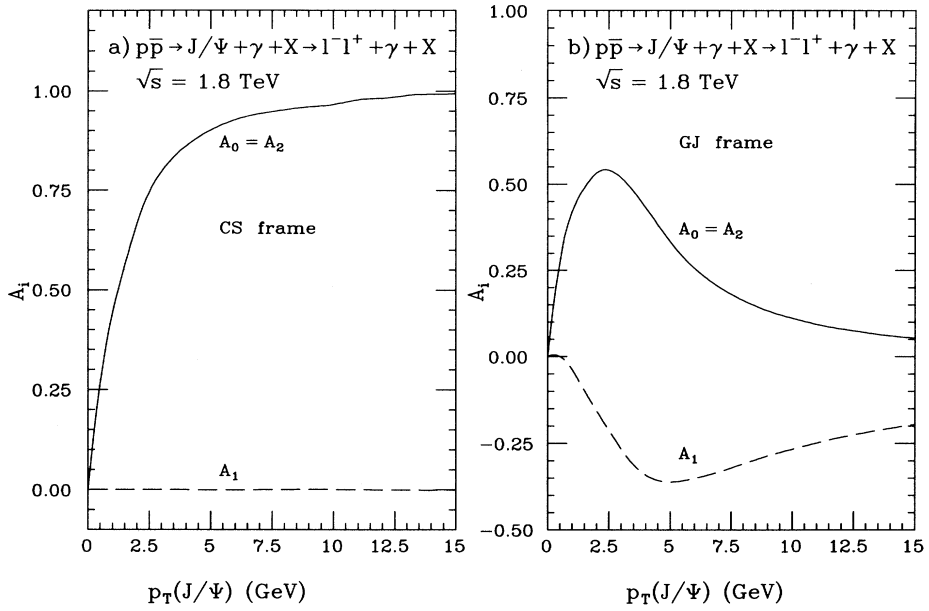

FIG. 4. Angular coefficients A_0, A_1, and A_2 for $J/\psi + \gamma$ production and decay in the CS frame (a) and GJ frame (b) as a function of the J/ψ transverse momentum at $\sqrt{S}$ = 1.8 TeV. No cuts have been applied.

no longer be described by the simple angular distribution in Eq. (29).

Figures 6–11 show the normalized ϕ and $\cos\theta$ distributions for the leptons in the CS and GJ frame for three different bins in the transverse momentum of the J/ψ. To demonstrate the effects of acceptance cuts, results are shown first without cuts and then with typical acceptance cuts imposed to the leptons and the photon.

Figures 6 and 7 show the ϕ and $\cos\theta$ distributions in the CS and GJ frame without cuts. The curves in Figs. 6 and 7 can be obtained from the results in Fig. 4 using the coefficients α and β defined in Eqs. (30) and (32). One observes a fairly strong ϕ dependence both in the CS [Fig. 6(a)] and the GJ [Fig. 7(a)] frame for the three $p_t(J/\psi)$ bins, which is expected from $\beta = A_2/4$ and the results in Fig. 4. The ϕ dependence is larger for high $p_T(J/\psi)$ bins in the CS frame, whereas an opposite behavior is found for the GJ frame. The coefficient α in Eq. (30) is negative for the three bins in the CS frame and positive in the GJ frame. The corresponding $\cos\theta$ distributions are therefore decreasing [increasing] with $\cos\theta$ in the CS [Fig. 6(b)] [GJ (Fig. 7(b)] frame. Let us recall that the angular distributions in Figs. 6 and 7 are determined by the polarization of the J/ψ with respect to the z axis in the CS and GJ frame [see Eq. (A9)].

Figures 8 and 9 show the ϕ and $\cos\theta$ distributions in

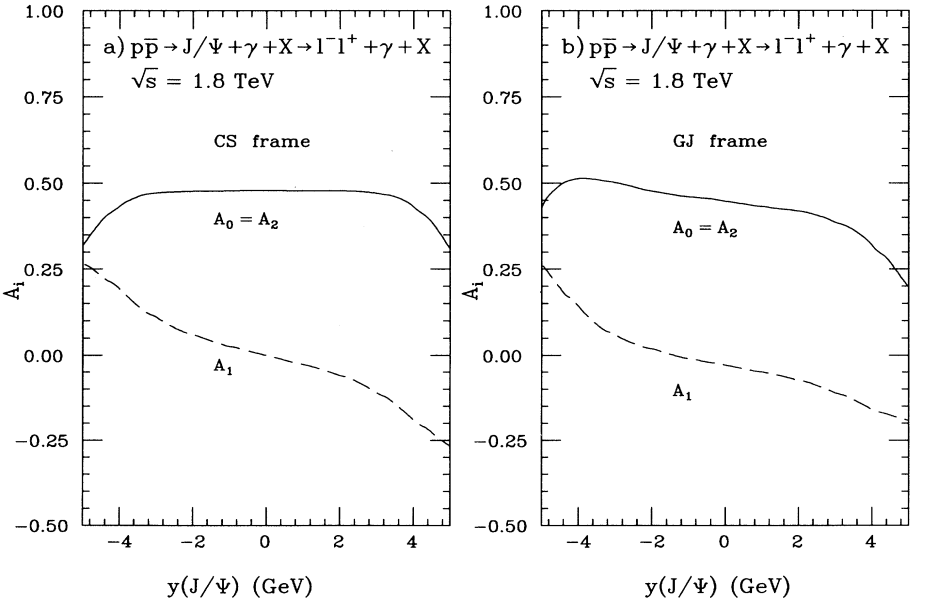

FIG. 5. Same as Fig. 4 for the $y(J/\psi)$ distribution.

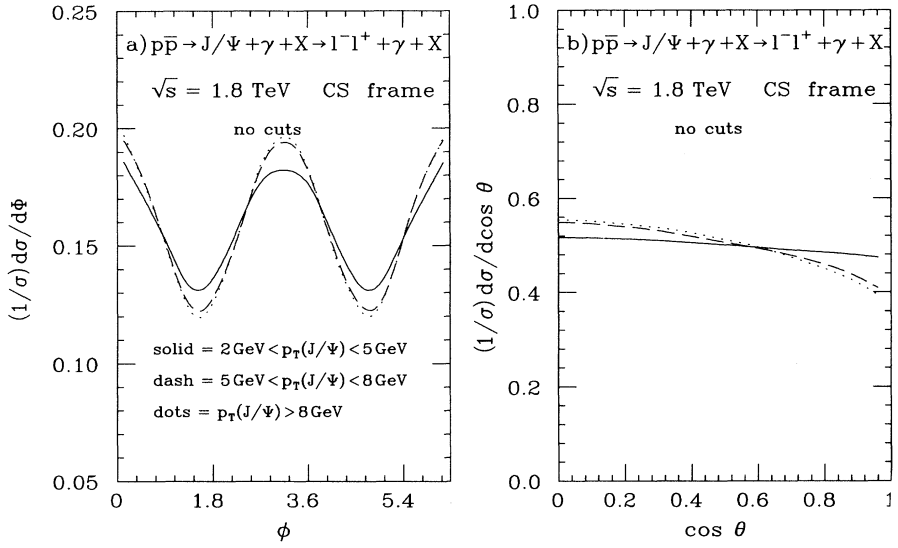

FIG. 6. (a) Normalized ϕ and (b) normalized $\cos\theta$ distributions of the leptons from J/ψ decay in the CS frame. Results are shown for three bins in $p_T(J/\psi)$: 2 GeV $< p_T(J/\psi) <$ 5 GeV (solid), 5 GeV $< p_T(J/\psi) <$ 8 GeV (dashed), 8 GeV $< p_T(J/\psi)$ (dotted). No cuts have been applied.

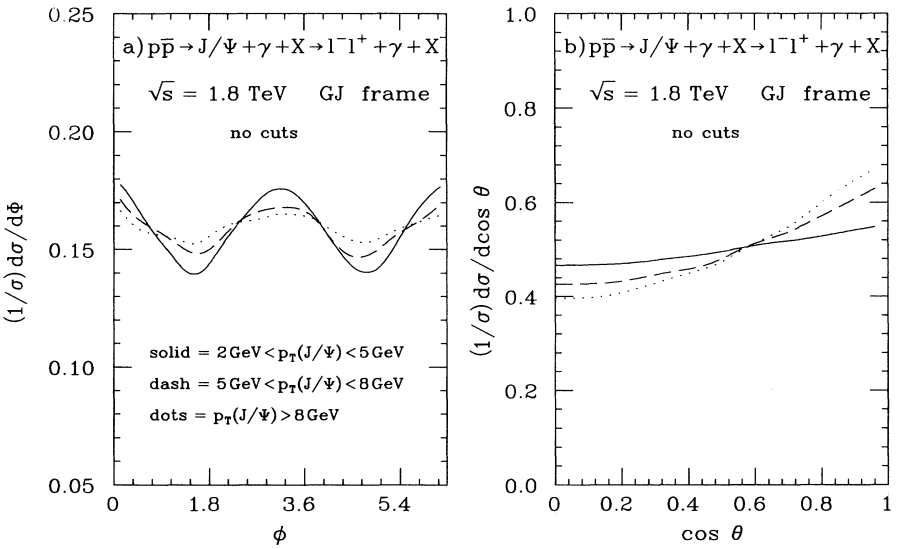

FIG. 7. Same as Fig. 6 in the GJ frame.

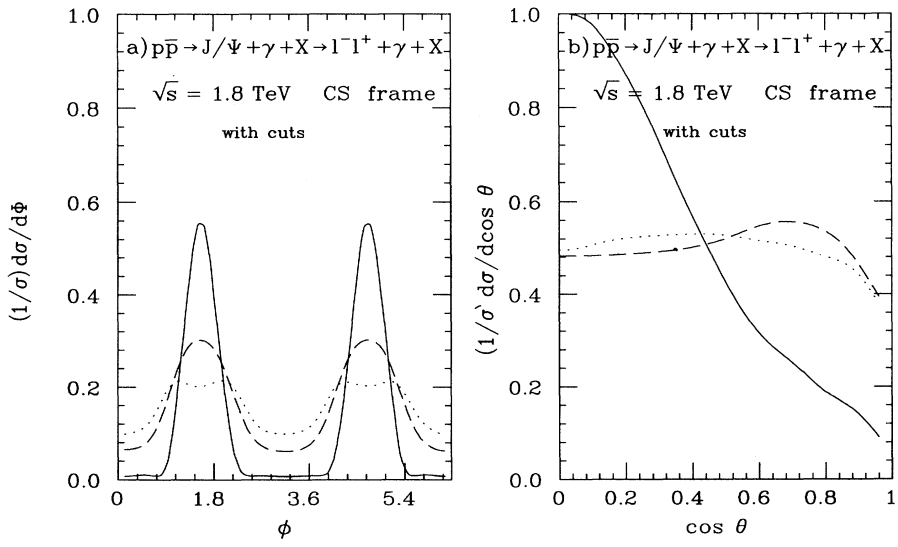

FIG. 8. Same as Fig. 6 but with the cuts $|y(\gamma, l^-, l^+)| < 2.5$, $p_T(l^-, l^+) > 1.8$ GeV.

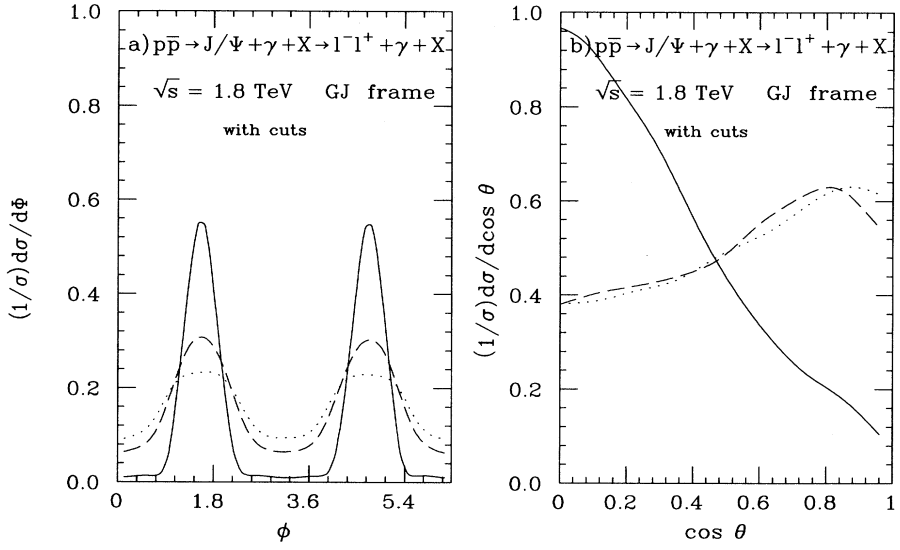

FIG. 9. Same as Fig. 7 but with the cuts $|y(\gamma, l^-, l^+)| < 2.5$, $p_T(l^-, l^+) > 1.8$ GeV.

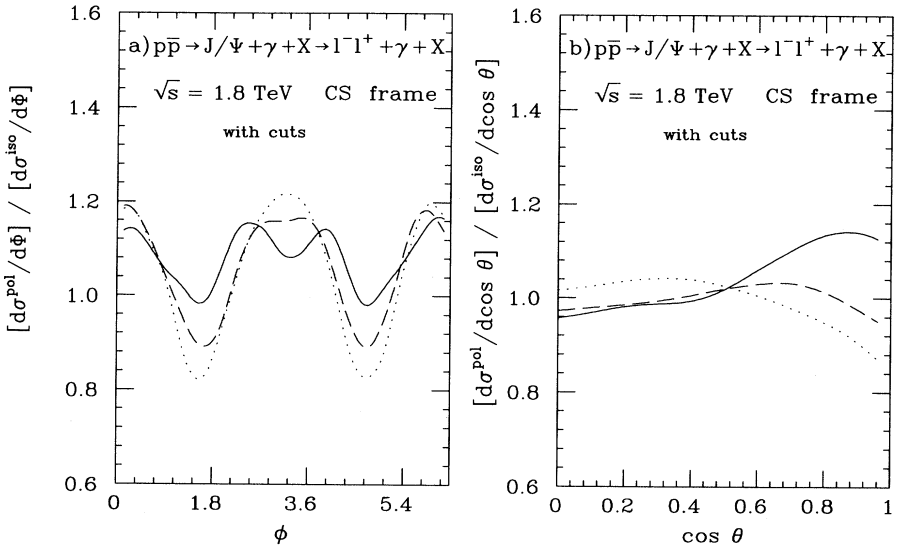

FIG. 10. Ratios of distributions obtained with full polarization effects to those obtained with isotropic decay of the J/ψ. Parts (a) and (b) are the ratios for the ϕ and $\cos\theta$ distributions in the CS frame, respectively. The cuts $|y(\gamma, l^-, l^+)| < 2.5, p_T(l^-, l^+) > 1.8$ GeV are included.

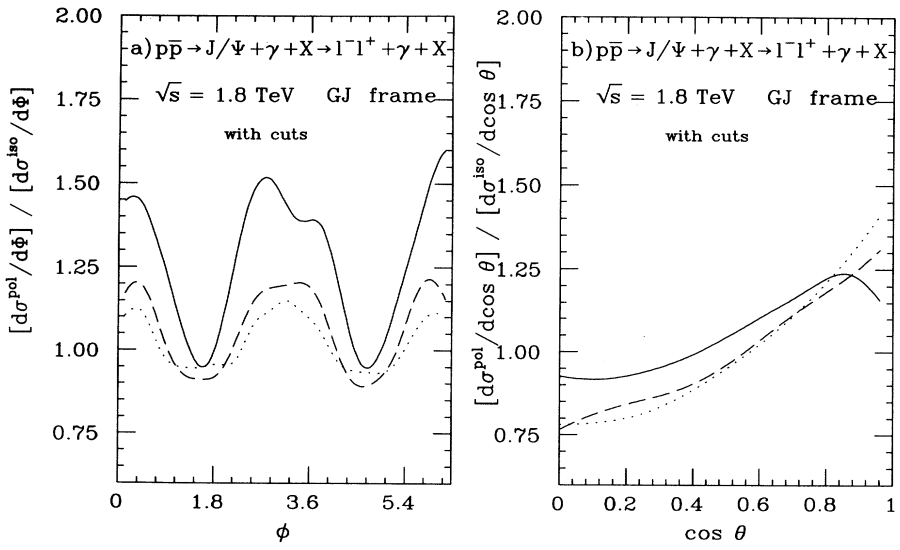

FIG. 11. Same as Fig. 10 for the GJ frame.

the CS and the GJ frame for the same bins in $p_T(J/\psi)$ as in Figs. 6 and 7 but with the cuts

$$p_T(l^-, l^+) > 1.8\,\text{GeV}, \qquad |y(\gamma, l^-, l^+)| < 2.5. \quad (39)$$

The cuts have a dramatic effect on the shapes of the distribution. The shapes of the distributions are now governed by the kinematics of the surviving events.[2] The cuts, which are applied in the laboratory frame, introduce a strong ϕ and $\cos\theta$ dependence. The cuts remove mainly events around $\phi = 0, \pi, 2\pi$ [Figs. 8 and 9(a)] and $\cos\theta > 0.5$ for the low $p_T(J/\psi)$ bin [solid line in Figs. 8 and 9(b)]. The ϕ distributions in Figs. 8 and 9(a) are very different from the "dynamical" ϕ distribution in Figs. 6 and 7(a) and there is only very little sensitivity to the polarization dependence (shown in Figs. 6 and 7) left in Figs. 8 and 9.

We have also analyzed the effect of the cuts separately by using the correct matrix element for J/ψ production, but with isotropic decay of the J/ψ, *i.e.*, neglecting spin correlations between J/ψ production and decay. The angular distributions in this case are very similar to the ones shown in Figs. 8 and 9 for the full matrix element.

In Figs. 10 and 11 we show ratios of the ϕ and $\cos\theta$ distributions in the CS and GJ frame for the same bins in $p_T(J/\psi)$ as in Figs. 6–9; the distribution with full polarization has been divided by the distribution obtained with isotropic decay of the J/ψ. Cuts are included in both cases. The large effects from the cuts are expected to almost cancel in this ratio.[3] In fact, we nearly recover the ϕ and $\cos\theta$ dependence of Figs. 6 and 7 in Figs. 10 and 11. Especially, the two high $p_T(J/\psi)$ bins (dashed and dotted lines in Figs. 10 and 11) contain most of the polarization dependence seen in Figs. 6 and 7. Comparing the results in the CS (Figs. 10 and 6) and the GJ frame (Figs. 11 and 7), the ratios in the CS frame are more sensitive to the ϕ distribution, whereas the ratios in the GJ frame are more sensitive to the $\cos\theta$ distribution, when cuts are applied.

Therefore, to regain sensitivity to the polarization effects in the presence of large kinematic cuts, we propose to divide the experimental distributions by the Monte Carlo distributions obtained using isotropic J/ψ decay.

IV. SUMMARY

Hadronic $J/\psi + \gamma$ production has been evaluated in the nonrelativistic bound state model. In leading order this final state can only be produced by gluon fusion. Analytical formula for the decay lepton distributions in terms of four structure functions are presented. If no cuts are applied, the angular distribution in the J/ψ rest frame is determined by the polarization of the J/ψ. We present Monte Carlo studies of the leptonic decay products of high p_T J/ψ's produced in association with a photon, when cuts are imposed on the photon and leptons. When acceptance cuts are imposed on the leptons, the angular distributions are dominated by kinematical effects rather than polarization effects. Polarization effects can be maximized by minimizing the cuts. Alternatively, it may be possible to retain J/ψ polarization effects by "dividing out" the kinematic effects, i.e., if the histogrammed data are divided by the theoretical result for isotropic J/ψ decay.

ACKNOWLEDGMENTS

We thank V. Barger and R.J.N. Phillips for insight regarding the effects of the cuts on the angular distributions. We thank J. Ohnemus, W.J. Stirling, and D. Summers for useful discussions. The work of C.S.K. was supported in part by the Korea Science and Engineering Foundation, in part by Non-Direct-Research-Fund, Korea Research Foundation 1993, in part by the Center for Theoretical Physics, Seoul National University, and in part by the Basic Science Research Institute Program, Ministry of Education, 1994, Project No. BSRI-94-2425. The work of E.M. was supported in part by the U.S. Department of Energy under Contract Nos. DE-AC02-76ER00881 and DE-FG03-91ER40674, by Texas National Research Laboratory Grant No. RGFY93-330, and by the University of Wisconsin Research Committee with funds granted by the Wisconsin Alumni Research Foundation.

APPENDIX A: STRUCTURE FUNCTIONS AND HELICITY CROSS SECTIONS

In this appendix, we will derive the partonic helicity cross section in Eqs. (17)–(25) for the production of polarized J/ψ's

The production cross section for

$$g(p_1) + g(p_2) \to J/\psi(P) + \gamma(k)\,, \quad (A1)$$

is

$$d\hat{\sigma} = \frac{1}{2s}|M|^2 dPS^{(2)}\,,$$

with

$$dPS^{(2)} = \frac{1}{8\pi s}\delta(s + t + u - P^2)\,dt\,du\,. \quad (A2)$$

The amplitude which describes the coupling of the γgg to the J/ψ can be calculated within the bound state formalism [6] to be

$$A^{gg\gamma} = \frac{1}{2}\frac{1}{\sqrt{4\pi M_\psi}} R(0)\,\text{Tr}\left[\mathcal{O}^0(\not{P} - M_\psi)(-\not{P})\right]\,, \quad (A3)$$

where $R(0)$ denotes the radial wave function of the bound

[2] We thank V. Barger and R. J. N. Phillips for pointing out this fact.

[3] Analogous ratios have been recently applied in [16] to regain the sensitivity to polarization effects in W and Z production in hadronic collisions.

state, which can be calculated either from potential models or can be related to the leptonic decay rate

$$|R(0)|^2 = \frac{M_\psi^2}{4\alpha^2(2/3)^2}\Gamma_{ee} \,. \tag{A4}$$

In Eq. (A3) E denotes the J/ψ polarization. The amplitude $\mathcal{O}^0$ can be obtained from the amplitude for the gluon-gluon fusion into a free quark pair at threshold and a photon:

$$\mathcal{O}^0 = \frac{-1}{4}\left[\frac{\not\varepsilon_1(\not P - 2\not p_1 + m_\Psi)\not\varepsilon^*(-\not P + 2\not p_2 + m_\Psi)\not\varepsilon_2}{Pp_1\ Pp_2} + \frac{\not\varepsilon^*(-\not P + 2\not p_1 + 2\not p_2 + m_\Psi)\not\varepsilon_1(-\not P - 2\not p_2 + m_\Psi)\not\varepsilon_2}{(Pp_1 + Pp_2 - 2p_1p_2)\ Pp_2}\right.$$
$$\left. + \frac{\not\varepsilon_1(\not P - 2\not p_1 + m_\Psi)\not\varepsilon_2(\not P - 2\not p_1 - 2\not p_2 + m_\Psi)\not\varepsilon^*}{Pp_1\ (Pp_1 + Pp_2 - 2p_1p_2)}\right] + [1 \leftrightarrow 2] \,. \tag{A5}$$

Here $p_1, p_2, \varepsilon_1, \varepsilon_2$ are the momenta and polarization vectors of the two gluons, and ε is the polarization vector of the photon. Coupling constants, spin average factors, and color matrices contribute a factor $(4\pi\,\alpha_s\,e\,2/3)^2(1/4)(2/3)$ to production cross section. After summing over the polarizations $\varepsilon_{1\alpha}, \varepsilon_{2\beta}, \varepsilon_\mu$ we define the density matrix elements of the J/ψ as

$$H^{\sigma\sigma'} = E_\delta(\sigma)T^{\delta\delta'}E^*_{\delta'}(\sigma') \,, \tag{A6}$$

where the hadronic tensor $T^{\delta\delta'}$ is

$$T^{\delta\delta'} = \frac{1}{2048{m_\psi}^2}\ \mathrm{Tr}\left[\mathcal{O}^{\alpha\,\mu\,\beta}(\not P - m_\psi)\gamma^\delta\right]\mathrm{Tr}\left[\mathcal{O}_{\alpha\,\mu\,\beta}(\not P - m_\psi)\gamma^{\delta'}\right]^* \,, \tag{A7}$$

and

$$E_\delta(\pm) = \frac{1}{\sqrt{2}}\,(0; \pm 1, -i, 0) \,,$$
$$E_\delta(0) = (0; 0, 0, 1) \,, \tag{A8}$$

are the polarization vectors for the J/ψ defined with respect to some coordinate axis in its rest frame (see below).

The angular dependence of the decay leptons from the J/ψ can be extracted by introducing the following linear combinations of the density matrix elements (we follow the technique presented in Appendix C of [8]):

$$H^{U+L} = H^{00} + H^{++} + H^{--} \,,$$
$$H^L = H^{00} \,,$$
$$H^T = \frac{1}{2}(H^{+-} + H^{-+}) \,, \tag{A9}$$
$$H^I = \frac{1}{4}\left(H^{+0} + H^{0+} - H^{-0} - H^{0-}\right) .$$

Collecting all remaining factors, one has

$$\frac{sd\sigma}{dt\,du} = \frac{16\pi\alpha\alpha_s^2 m_\psi}{27s}|R(0)|^2\ \{(1+\cos^2\theta)\ H^{U+L} + (1 - 3\cos^2\theta)\ H^L$$
$$+2\sqrt{2}\sin 2\theta\cos\phi\ H^I + 2\sin^2\theta\cos 2\phi\ H^T\}\delta(s + t + u - P^2) \,. \tag{A10}$$

In Eq. (A10) θ and ϕ denotes the lepton angles in the lepton pair rest frame. What remains is the calculation of the H^α in the CS and GJ frame.

For this purpose we choose a specific representation for $E_\delta(\sigma)E^*_{\delta'}(\sigma')$ in Eq. (A6) and express them in terms of of $g_{\delta\delta'}, P_\delta P_{\delta'}, p_{i\,\delta}p_{j\,\delta'}$ $(i,j = 1,2)$. Let us define the covariant projections

$$\tilde{T}^\beta \equiv \mathcal{P}^\beta_{\delta\delta'}\,H^{\delta\delta'} \quad (\beta \in \{U+L, L_1, L_2, L_{12}\}) \,, \tag{A11}$$

where

$$\mathcal{P}^{U+L}_{\delta\delta'} = -\hat{g}_{\delta\delta'} ,$$
$$\mathcal{P}^{L_1}_{\delta\delta'} = \frac{1}{\hat{E}_1^2}\,\hat{p}_{1\delta}\hat{p}_{1\delta'} ,$$
$$\mathcal{P}^{L_2}_{\delta\delta'} = \frac{1}{\hat{E}_2^2}\,\hat{p}_{2\delta}\hat{p}_{2\delta'} , \tag{A12}$$
$$\mathcal{P}^{L_{12}}_{\delta\delta'} = \frac{1}{\hat{E}_1\hat{E}_2}\,(\hat{p}_{1\delta}\hat{p}_{2\delta'} + \hat{p}_{1\delta'}\hat{p}_{2\delta}) .$$

We have introduced the tensors with carets:

$$\hat{g}_{\delta\delta'} = g_{\delta\delta'} - \frac{P_\delta P_{\delta'}}{P^2} , \qquad \hat{p}_{i,\delta} = p_{i\,\delta} - \frac{p_i P}{P^2} p_{i\,\delta} ,$$
$$\hat{E}_1 = \frac{P^2 - t}{2\sqrt{P^2}} \qquad \hat{E}_2 = \frac{P^2 - u}{2\sqrt{P^2}} . \tag{A13}$$

The helicity structure functions H^α in Eq. (A10) for a given J/ψ rest frame are linear combinations of the covariant projections in Eq. (A11).

For the CS frame one has [8]

$$\begin{pmatrix} H^{U+L} \\ H^L \\ H^T \\ H^I \end{pmatrix}_{\rm CS} = \begin{pmatrix} 1 & 0 & 0 & 0 \\ 0 & \frac{1}{4\cos^2\gamma_{\rm CS}} & \frac{1}{4\cos^2\gamma_{\rm CS}} & \frac{-1}{4\cos^2\gamma_{\rm CS}} \\ \frac{1}{2} & -\frac{(1+\cos^2\gamma_{\rm CS})}{8\sin^2\gamma_{\rm CS}\cos^2\gamma_{\rm CS}} & -\frac{(1+\cos^2\gamma_{\rm CS})}{8\sin^2\gamma_{\rm CS}\cos^2\gamma_{\rm CS}} & \frac{(1-3\cos^2\gamma_{\rm CS})}{8\sin^2\gamma_{\rm CS}\cos^2\gamma_{\rm CS}} \\ 0 & \frac{1}{4\sqrt{2}\sin\gamma_{\rm CS}\cos\gamma_{\rm CS}} & \frac{-1}{4\sqrt{2}\sin\gamma_{\rm CS}\cos\gamma_{\rm CS}} & 0 \end{pmatrix} \begin{pmatrix} H^{U+L} \\ H^{L_1} \\ H^{L_2} \\ H^{L_{12}} \end{pmatrix} , \tag{A14}$$

where

$$\cos\gamma_{\rm CS} = \sqrt{\frac{m_\psi{}^2 s}{(t-m_\psi{}^2)(u-m_\psi{}^2)}} , \qquad \sin\gamma_{\rm CS} = -\sqrt{1-\cos^2\gamma_{\rm CS}} . \tag{A15}$$

The explicit results for $H^\alpha_{\rm CS}$ are given in Eqs. (18)–(21).

The results for the GJ frame can be obtained from

$$\begin{pmatrix} H^{U+L} \\ H^L \\ H^T \\ H^I \end{pmatrix}_{\rm GJ} = \begin{pmatrix} 1 & 0 & 0 & 0 \\ 0 & 1 & 0 & 0 \\ \frac{1}{2} & -\frac{(1+\cos^2\gamma_{\rm GJ})}{2\sin^2\gamma_{\rm GJ}} & -\frac{1}{\sin^2\gamma_{\rm GJ}} & \frac{\cos\gamma_{\rm GJ}}{\sin^2\gamma_{\rm GJ}} \\ 0 & \frac{-\cos\gamma_{\rm GJ}}{\sqrt{2}\sin\gamma_{\rm GJ}} & 0 & \frac{1}{2\sqrt{2}\sin\gamma_{\rm GJ}} \end{pmatrix} \begin{pmatrix} H^{U+L} \\ H^{L_1} \\ H^{L_2} \\ H^{L_{12}} \end{pmatrix} \tag{A16}$$

and

$$\cos\gamma_{\rm GJ} = 1 - \frac{2m_\psi{}^2 s}{(t-m_\psi{}^2)(u-m_\psi{}^2)} , \qquad \sin\gamma_{\rm GJ} = -\sqrt{1-\cos^2\gamma_{\rm GJ}} . \tag{A17}$$

The explicit results for $H^\alpha_{\rm GJ}$ are given in Eqs. (22)–(25).

[1] UA1 Colloration, C. Albajar *et al.*, Phys. Lett. B **256**, 112 (1991).

[2] CDF Colloration, F. Abe *et al.*, Phys. Rev. Lett. **69**, 3704 (1992).

[3] R. Baier and R. Rückl, Z. Phys. C **19**, 251 (1983); F. Halzen, F. Herzog, E.W.N. Glover, and A.D. Martin, Phys. Rev. D **30**, 700 (1984); B. van Eijk and R. Kinnunen, Z. Phys. C **41**, 489 (1988); E.W.N. Glover, A.D. Martin, and W.J. Stirling, *ibid.* **38**, 473 (1988).

[4] E. Braaten and T.C. Yuan, Phys. Rev. Lett. **71**, 993 (1993); M.A. Doncheski, S. Fleming, and M.L. Mangano in *Proceedings of the Workshop on Physics at Current Accelerators and the Supercolliders,* Argonne, Illinois, edited by J. Hewett, A.R. White, and D. Zeppenfeld (Ar-

gonne Report No. 93-92, Argonne, 1993); E. Braaten, K. Cheung and T.C. Yuan, Phys. Rev. D **48**, 4230 (1993); M. Cacciari and M. Greco, Phys. Rev. Lett. **73**, 1586 (1994); E. Braaten, M.A. Doncheski, S. Fleming, and M.L. Mangano, Phys. Lett. B **333**, 548 (1994).

[5] D.P. Roy and K. Sridhar, Report No. CERN-TH.7371/94, 1994 (unpublished).

[6] E.L. Berger, D. Jones, Phys. Rev. D **23**, 1521 (1981); J.H. Kühn, J. Kaplan, and E.G.O. Safiani, Nucl. Phys. **B157**, 125 (1979; B. Guberina, J.H. Kühn, R.D. Peccei, and R. Rückl, *ibid.* **B174**, 317 (1980).

[7] J.C. Collins and D.E. Soper, Phys. Rev. D **16**, 2219 (1977);

[8] E. Mirkes, Nucl. Phys. **B387**, 3 (1992).

[9] P. Cho, M.B. Wise, and S.P. Trivedi, Phys. Rev. D **51**, R2039 (1995); P. Cho and M.B. Wise, *ibid.* **51**, 3352 (1995); Report No. CALT-68-1962, 1994 (unpublished).

[10] M. Drees and C.S. Kim, Z. Phys. C **53**, 673 (1992); C.S. Kim and E. Reya, Phys. Lett. B **300**, 298 (1993); M.A. Doncheski and C.S. Kim, Phys. Rev. D **49**, 4463 (1994).

[11] V.D. Driesen, H.J. Kühn, and E. Mirkes, Phys. Rev. D **49**, 3197 (1994).

[12] E.L. Berger and D. Jones, Phys. Rev. D **23**, 1521 (1981).

[13] M. Glück, E. Reya, and A. Vogt, Z. Phys. C **53**, 127 (1992);

[14] NMC Colloration, D. Allasia *et al.*, Phys. Lett. B **258**, 493 (1991).

[15] C.S. Lam and W.-K. Tung, Phys. Rev. D **18**, 2447 (1978); **21**, 2712 (1980); Phys. Lett. **80B**, 228 (1979); K. Kajantie, J. Lindfors, and R. Raitio, *ibid.* **74B**, 384 (1978); Nucl. Phys. **B144**, 422 (1978); J. Cleymans and M. Kuroda, Phys. Lett. **80B**, 385 (1979); Nucl. Phys. **B155**, 480 (1979);

[16] E. Mirkes and J. Ohnemus, Phys. Rev. D **50**, 5692 (1994).